

HARPO: beam characterization of a TPC for gamma-ray polarimetry and high angular-resolution astronomy in the MeV-GeV range

Shaobo Wang

LLR, Ecole Polytechnique, CNRS/IN2P3, France

E-mail: wang@llr.in2p3.fr

Denis Bernard, Philippe Bruel, Mickael Frotin, Yannick Geerebaert, Berrie Giebels, Philippe Gros, Deirdre Horan, Marc Louzir, Patrick Poilleux, Igor Semeniouk

LLR, Ecole Polytechnique, CNRS/IN2P3, France

David Attié, Denis Calvet, Paul Colas, Alain Delbart, Patrick Sizun

Irfu, CEA-Saclay, France

Diego Götz

AIM, CEA/DSM-CNRS-Université Paris Diderot, France

Irfu/Service d'Astrophysique, CEA-Saclay, France

Sho Amano, Takuya Kotaka, Satoshi Hashimoto, Yasuhito Minamiyama, Akinori Takemoto, Masashi Yamaguchi, Shuji Miyamoto

LASTI, University of Hyôgo, Japan

Schin Daté, Haruo Ohkuma

JASRI/SPring8, Japan

Abstract. A time projection chamber (TPC) can be used to measure the polarization of gamma rays with excellent angular precision and sensitivity in the MeV-GeV energy range through the conversion of photons to e^+e^- pairs.

The Hermetic ARGON Polarimeter (HARPO) prototype was built to demonstrate this concept. It was recently tested in the polarized photon beam at the NewSUBARU facility in Japan. We present this data-taking run, which demonstrated the excellent performance of the HARPO TPC.

1. Introduction

Gamma-ray astronomy is the primary means by which we can study the non-thermal processes occurring in cosmic sources such as active galactic nuclei (AGN), pulsars and gamma-ray bursts (GRBs) [1]. The ability to measure the linear polarization in this energy range would provide a powerful diagnostic for the understanding of the physical processes at work in these sources [2]. A telescope with the ability to perform polarimetry above 1 MeV has never been flown in space [3]. Gamma-ray telescopes have improved in sensitivity and resolution from COS-B [4] to the Fermi-LAT [5], but the performance of these pair-creation telescopes decreases at low energy where the background is problematic and the angular resolution is limited by multiple scattering.

The performance and polarimetry potential of a TPC have been studied in detail in Ref. [6] and [7]. Several effects contribute to the angular resolution, which is shown as a function of photon energy in Fig. 1 for an argon gas TPC. The angular resolution for pair production is limited by multiple scattering of the electrons in the gas. Also, most conversions take place in the field of a nucleus whose recoil momentum is impossible to measure because of the very short recoil path length. This puts a limit on the resolution at energies < 100 MeV. Even with these limitations however, an improvement in angular momentum of up to an order of magnitude with respect to that of the Fermi-LAT is achievable with a TPC.

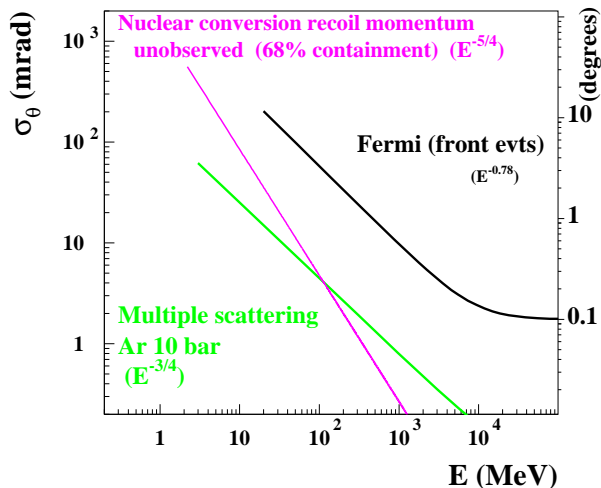


Figure 1. Various contributions to the angular resolution of a TPC gamma telescope as a function of the photon energy [6], compared to that of the Fermi-LAT [5]. The multiple scattering contribution (green) is given for a 10 bar argon TPC, using an optimal tracking such as that implemented in a Kalman filter, and with a track sampling of 1 mm and a spatial resolution of 0.1 mm. At high energies (> 100 MeV), it is limited by the multiple scattering of the electrons in the gas. At lower energies, it is constrained by the unknown recoil momentum of the nucleus. This limit can be overcome by looking at triplet conversion, but they are rarer and more difficult to reconstruct.

The polarimetry of cosmic sources with a pair-creation telescope has long been considered to be difficult or even impossible, as thick, high- Z detector elements are needed to convert the incoming photon, and the conversion electrons then undergo multiple scattering in the converter, after which the information about the azimuthal angle of the conversion plane is blurred [8]. We have built and validated an event generator [7] which is full (5D, either nuclear or triplet conversion) exact down to threshold and polarized. We have characterized the properties of a telescope based on a thin homogeneous detector with optimal tracking and have established

the power laws that describe the dominating contributions to the angular resolution [6]. For such a detector, even when the dilution of the effective polarization asymmetry due to multiple scattering is taken into account, polarimetry can still be performed with high precision (still under the assumption of optimal tracking) [7].

The HARPO project aims to characterize the TPC technology as a high angular resolution polarimeter and telescope in the MeV-GeV range, enabling us to obtain unprecedented sensitivity for the detection of low-energy gamma rays. A TPC is a detector in which traversing charged particles ionize the detector material. The electrons produced drift along an electric field, E , and are then amplified and measured on the x - y readout plane. The drift time gives a measure of the z coordinate. HARPO would be the first space polarimeter above 1 MeV.

In this paper we first describe the demonstrator that we have built to validate the performance of the TPC technology, in particular the characterization of the GEM and micromegas combinations used for gas amplification ¹. Then we present the recent experimental campaign, in which the detector was exposed to the quasi-monochromatic and almost fully polarized beam provided by the BL01 line of the NewSUBARU facility, operated by the LASTI in University of Hyôgo in Japan.

2. The HARPO TPC demonstrator

The HARPO demonstrator [9] (Fig. 2) is a 30 cm cubic TPC which can be operated from low pressure up to 5 bar. It is surrounded by 6 scintillator plates that provide an external trigger. Amplification is performed with the combination of two GEMs [10] and one micromegas [11].

The readout comprises two series (x , y , perpendicular to each other) of 288 copper strips with 1 mm pitch. Signals are acquired with AFTER chips [12] using the Feminos system [13].

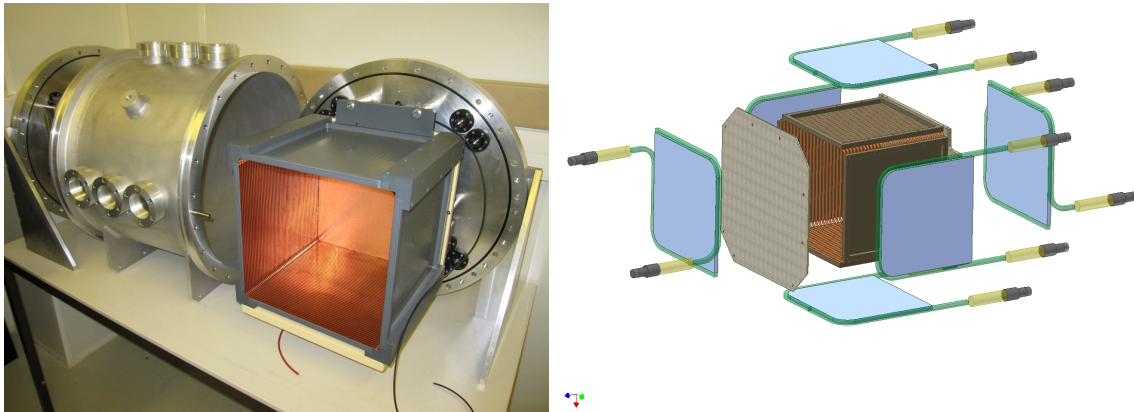


Figure 2. Left: the HARPO TPC demonstrator. Right: sketch of HARPO. A cubic TPC in the center, with a readout plane of micromegas and GEM on the left. Six scintillator plates, each equipped with a wavelength shifter and two photo-multipliers, are used for trigger. The system fits in an aluminum cylinder which can operate up to 5 bar pressure.

¹ The 2012 tests showed that with the 0.4 mm narrow collecting strips that we are using, the micromegas alone does not provide sufficient amplification at 4 bar for routine operation in a safe configuration [9]. We have therefore complemented the micromegas with two layers of Gas Electron Multiplier (GEM).

3. The HARPO amplification system

We first characterized the performance of the GEM+micromegas amplification system using a radioactive source. The amplification system was subsequently integrated into the TPC detector, where it was characterized using cosmic rays.

3.1. Characterization of micromegas and GEM(s) combinations with a radioactive source

We characterized the combination of a micromegas and either one or two GEM in a gas mixture (Ar:95 %Isobutane:5 %) at atmospheric pressure. This was done in a dedicated test setup using a ^{55}Fe source[16]. The successive amplification steps were kept at a distance of 2 mm from each other by spacers (Fig. 3 left).

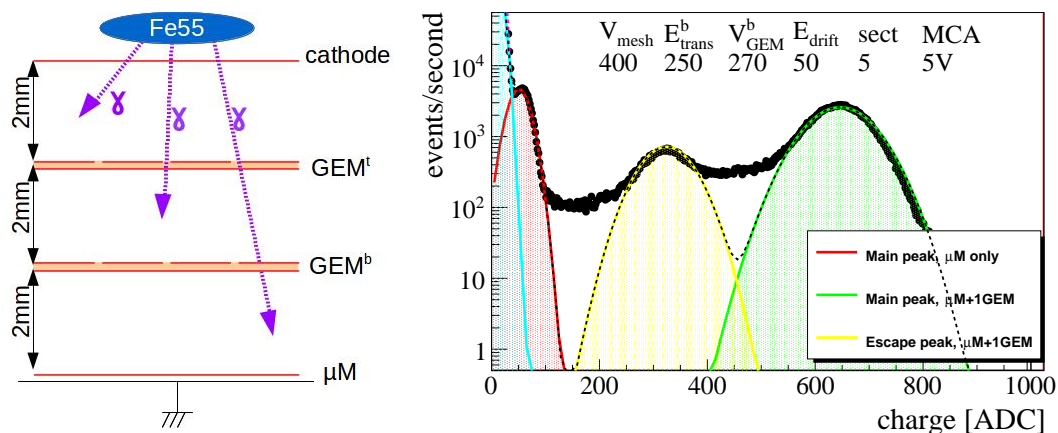


Figure 3. Left: the layout of the test setup, with one micromegas and two GEMs. (By applying a null or inverted voltage to the top GEM, we only observe conversion in the two lower regions). Right: an example of a measured ^{55}Fe spectrum from amplification with one micromegas and one GEM. The main peak (5.9 keV) is plotted after amplification with only the micromegas (red) or with both micromegas and GEM (green). The escape peak is only visible with full amplification (yellow).

In argon, the X-rays from a ^{55}Fe source deposit either 5.9 keV (main peak) or 2.7 keV (escape peak) upon ionization. This conversion can take place either above or below a given GEM sheet. The ionization electrons are therefore either amplified by that GEM or not. A typical spectrum is shown in Fig. 3 (right). The main and the escape peaks are seen with amplification from the micromegas and one GEM, and the main peak with micromegas amplification only. The ratio of the position of the two main peaks provides a precise measurement of the absolute GEM amplification gain. Further details on these measurements, including foil transparency and extraction efficiency, can be found in Ref. [16].

3.2. Characterization with cosmic rays

The system of micromegas and 2 GEMs was commissioned in the detector. It was tested with cosmic rays, using the same gas mixture at several pressures. Most cosmic muons are relativistic and therefore deposit the same average energy per unit length. The TPC was set "vertical", so that most cosmic rays entered it through the amplification system. We selected events with a cosmic ray that crossed the full z of 30 cm by triggering on the coincidence of the up and down scintillator signals.

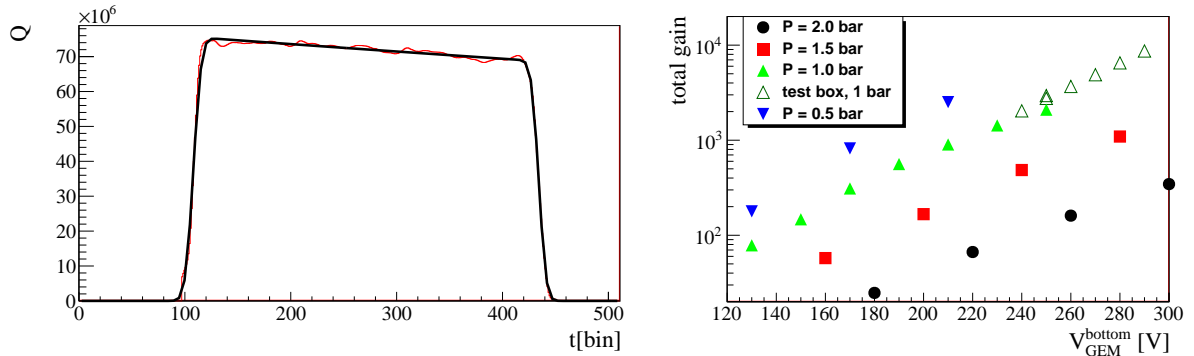


Figure 4. Left: average total charge per track as a function of time, for a run of cosmic rays that traversed the full TPC length, entering through the anode and exiting through the anode. We extract the drift velocity, the electron absorption per unit length and the amplification gain from such spectra. Right: the effective gain measured from cosmic rays in the TPC for several gas pressures. The results at 1 bar are consistent with those obtained with the radioactive source.

Table 1. Electron beam energy, laser wavelength, and γ -ray energy at the Compton edge obtained from these.

E_e^- [GeV]		0.618	0.982	1.233	1.480	Pulsing rate [kHz]	Polarization
Laser	λ [μm]	E_γ [MeV]					
Nd:YVO ₄ (2ω)	0.532	13.4	33.3	52.1	74.3	20	$P \approx 1$
Nd:YVO ₄ (1ω)	1.064	6.76	16.9	26.6	38.1	20	$P \approx 1$
Er(fiber)	1.540	4.68	11.8	18.5	26.5	200	$P = 0$
CO ₂	10.55		1.74	2.73	3.93	CW	$P = 0$

The charge distribution over drift time is shown in Fig. 4 (left). The value of the drift velocity, v_{drift} , was easily obtained using the basic relation of the TPC mechanism, $z = v_{\text{drift}} \times t_{\text{drift}}$, since the cosmic rays traverse the full z thickness of $L_{\text{TPC}} = 30$ cm. The slope of the plateau corresponds to electron absorption in the gas. The average charge per track for each run is used to estimate the amplification gain. From this spectrum, the drift velocity, the attenuation length and the total amplification gain were extracted. Fig. 4 (right) shows the amplification gain for several TPC gas pressures as a function of the voltage on one of the GEMs. The measurements are consistent with those obtained using the ^{55}Fe source.

4. Data-taking at NewSUBARU

In Nov. 2014 the detector was exposed to a beam of pseudo-monochromatic gamma-ray photons delivered by the BL01 beam line at NewSUBARU [15].

4.1. Laser-Compton Source (LCS)

The gamma-ray beam is produced by the inverse Compton scattering of laser photons by relativistic electrons. The electron beam energy can be varied in the range $0.6 \sim 1.5$ GeV. The laser beams available are: Nd:YVO₄ (2ω) with wavelength $\lambda = 0.532 \mu\text{m}$, Nd:YVO₄ (1ω) $\lambda = 1.064 \mu\text{m}$, Er (fiber) $\lambda = 1.540 \mu\text{m}$ and CO₂ $\lambda = 10.55 \mu\text{m}$. This results in a gamma energy range at the Compton edge between 1.7 MeV and 74 MeV as shown in Table 1. As the gamma

has a maximum energy for forward Compton scattering, energy selection was performed by using a collimator on axis. When collimation is applied, the polarisation of the laser beam is almost entirely transferred to the gamma beam: in that way, an almost fully polarized gamma beam ($P \approx 1$) is obtained. A general issue in polarization studies is the control of a possible systematic bias induced by the non-cylindrical-symmetric structure of the detector [17]. Therefore in addition to the fully polarized data, some data with a non polarized beam were taken. To produce such a beam, a $\lambda/4$ plate is used. This changes the linear polarization to circular polarization, which, as far as pair conversion is concerned, is equivalent to random polarization ($P = 0$). Or vice versa.

4.2. The HARPO Trigger system

For the previous characterizations using cosmic rays, the TPC was triggered on a simple coincidence of scintillator signals [9, 14]. In contrast, for data taking in beam, we wished to maximize the fraction of selected gammas that converted in the gas. Therefore a dedicated, more sophisticated trigger was designed. In addition it provides separately the control of the efficiency of each of its components.

4.2.1. Description of signals The HARPO trigger system is based on a PARISROC2 [19] chip mounted on a PMM2 [18] board. This trigger is built from the discriminated signals of the scintillators, laser and micromegas mesh as shown in Fig. 6. The available signals are:

- Laser: when a pulsed laser is used, the laser's trigger signal L (Fig. 5) is used. It also determines the time at which the event takes place, t_0 , with a precision of a few 10 ns.

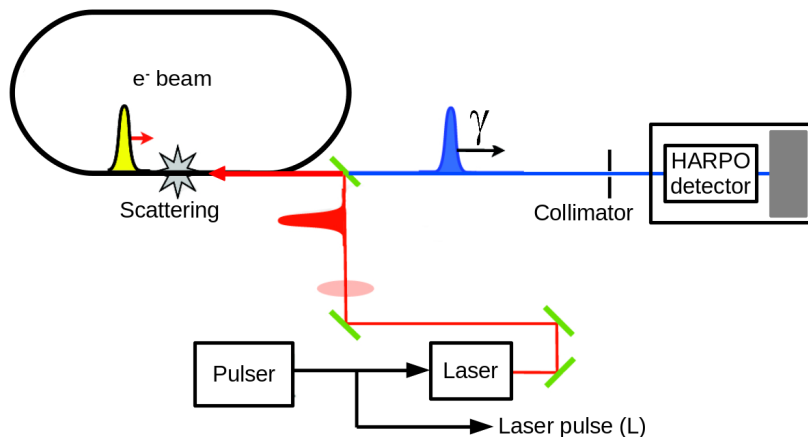


Figure 5. Schema of the Laser trigger used at NewSUBARU.

- Scintillator: the signal comes from 12 PMTs on 6 scintillators. The signal is recorded, whether there is a trigger or not. It gives t_0 with a hundred nanosecond precision. This signal determines t_0 when the laser signal is not available (CO_2).
- Micromegas mesh: the signal induced on the mesh is long and has an unpredictable shape: it corresponds to the time distribution of the charge deposited by the event in the TPC gas as it drifts towards the anode. The signal is amplified and derived through a 5 nF capacitor. It is then discriminated with a constant-fraction discriminator (CFD), so as to determine the rising edge t_{start} of the signal. The RC constant of the readout electronics of the mesh

signal is $\approx 1\mu\text{s}$. It has been fixed as a compromise between the amount of electronic noise given the large capacitance of the full mesh, of 8 nF, and the need of a precise determination of the rising edge of the signal t_{start} .

Events that have a too small of a delay between the time of the event, t_0 , and the discriminated mesh signal rising edge, t_{start} , are rejected. This provides a veto on background tracks created in the beam line upstream of the TPC and on gamma rays which converted in the material between the up scintillator and the active TPC gas (example: in the PCB supporting the amplification system).

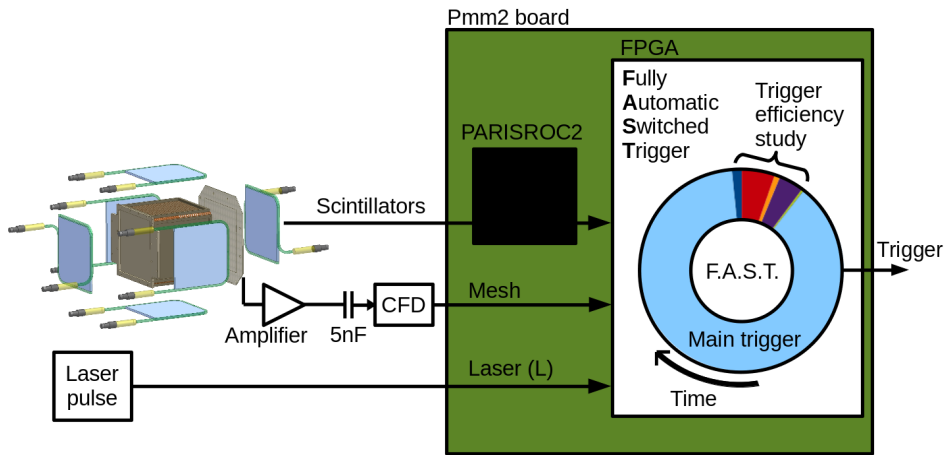


Figure 6. Global view of HARPO trigger system.

4.2.2. Gamma trigger line. The gamma trigger, T_γ , is designed so as to select gamma rays produced by LCS and that converted inside the TPC gas. The conditions are listed below:

- the upstream scintillator signal (S_{up}) is used as a veto,
- at least one downstream scintillator signal (O , other than “up”) is required,
- the laser trigger signal (L), when present, is used,
- the events with a signal present in the mesh are selected, vetoing the prompt part as already explained, we require $t_{\text{start}} - t_0 > 1\mu\text{s}$. This “slow” selection of a mesh signal is denoted M_{slow} .

The main γ trigger line is therefore defined as the combination of the four following components:

$$T_\gamma \equiv \bar{S}_{up} \cap O \cap M_{\text{slow}} \cap L \quad (1)$$

The distribution of t_{start} is shown in Fig. 8. Gamma conversions inside the TPC gas (blue) are the signal events. The flatness of that part of the spectrum is due to the fact that the probability of conversion per unit path length is constant for a thin detector. Tracks entering the detector from upstream and gamma conversions in the detector material upstream of the TPC gas, which escaped the vetos, form the (green) peak. If we had used a trigger without any veto, the height of this peak would have been larger by several orders of magnitude, precluding an efficient data taking. Events (red) which lie outside the normal time range (i.e., $t_{\text{start}} < 100$ or $t_{\text{start}} > 400$) are due to energy deposition inside the gas by events that are not related to the trigger (pile-up).

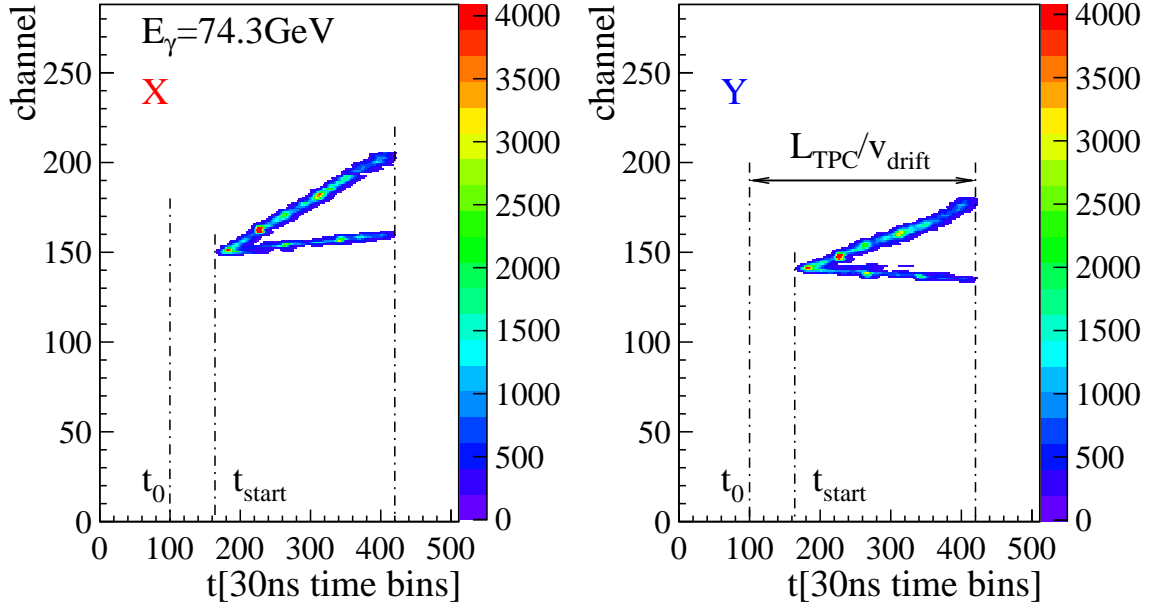


Figure 7. A gamma event that was selected by the gamma trigger, with definitions of timing information.

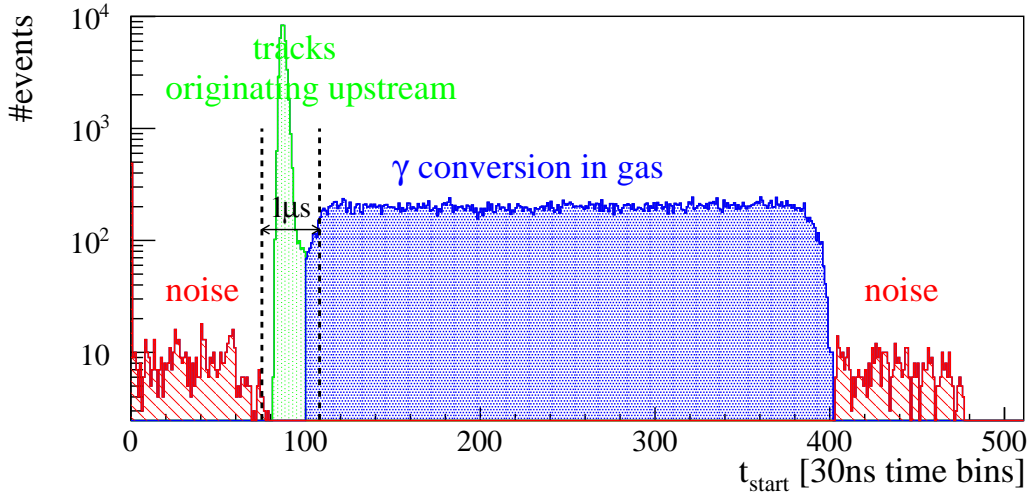


Figure 8. Distribution of event rising edge t_{start} for one run (all trigger lines): tracks originating upstream (green), gamma conversion inside the TPC gas (blue), charge deposition inside the gas by events not related to the trigger (red).

4.2.3. Other Trigger Lines. In addition to the main gamma trigger line, separate trigger lines have been formed with one of the trigger components omitted (such as $O \cap M_{\text{slow}} \cap L$, $\bar{S}_{\text{up}} \cap M_{\text{slow}} \cap L$, $\bar{S}_{\text{up}} \cap O \cap L$, $\bar{S}_{\text{up}} \cap O \cap M_{\text{slow}}$, in the case of a pulsed laser). Analysis of these specific data will enable us to control separately the signal efficiency and the background rejection factor for each component of the main trigger line. Other dedicated lines were used,

such as the “traversing z track” line for calibration purposes. Most of these additional lines were down-scaled so as to not saturate the bandwidth of the digitizing electronics, and were active only for a fraction of the time, as denoted by the rainbow part of Fig. 6. Approximately 90% of the time was devoted to the main trigger line.

4.3. Gas

The pressure vessel was evacuated down to $\sim 2 \times 10^{-6}$ bar, rinsed with ~ 0.1 bar gas, evacuated again, and then filled with 2.1 bar of the gas mixture (Ar:95 % Isobutane:5 %). This same gas was used in a sealed mode for 23 days.

At the end of the data taking, a pressure scan from 1 to 4 bar was performed, with the gas amplification tuned so that the signal amplitude was kept constant ($E_e = 1.5$ GeV, $N_d = 1\omega$, $P = 1$).

4.4. Monitoring

During data taking in the beam, some basic parameters were monitored, such as alignment, amplification gain, trigger performance and event quality after some very basic tracking.

4.4.1. Alignment. The alignment of the HARPO detector in the collimated gamma beam was monitored by plotting the transverse (x or y) position of the gamma conversion candidate vertex as a function of its longitudinal position z (Fig. 9). The vertex is defined here from the charge-weighted barycenter of the three first clusters of a selected gamma-conversion event (triggered by the gamma trigger).

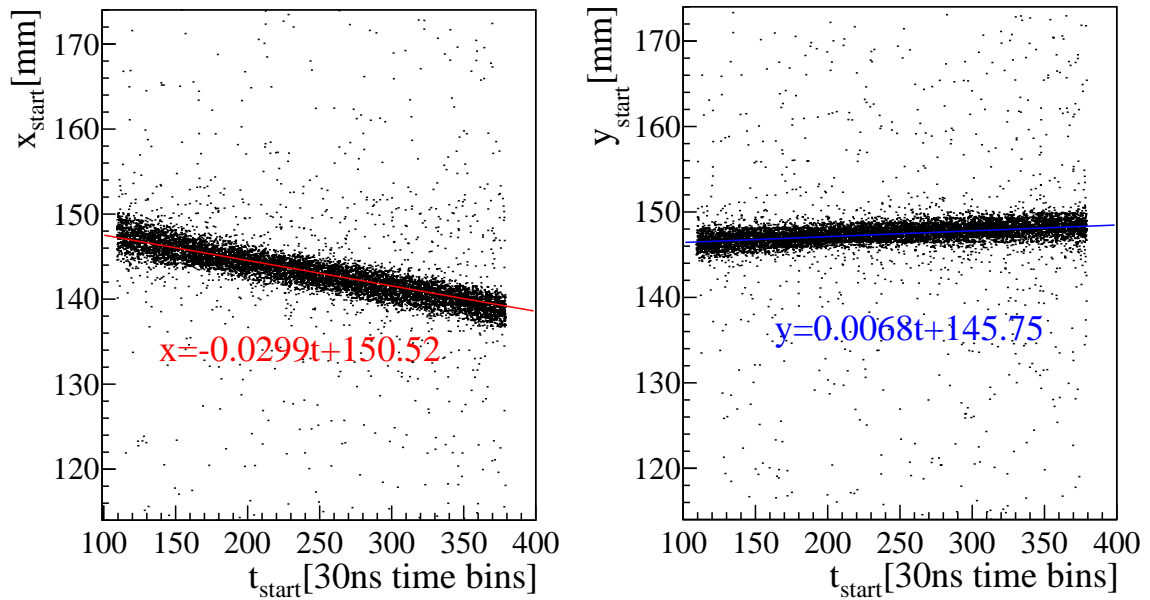


Figure 9. Alignment plot for run 1277 (1 mm diameter collimator), with linear fit (gamma trigger line).

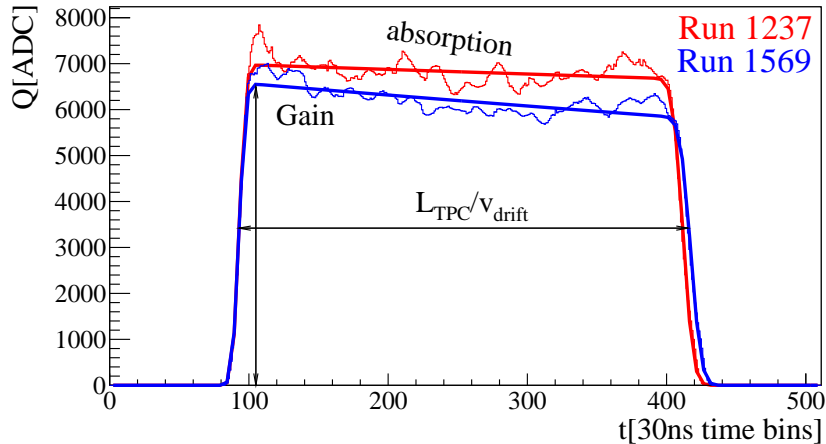


Figure 10. The average energy deposited at each time bin per traversing track along the z -axis for two runs separated by a full week of high flux running.

4.4.2. Calibration. The calibration of the TPC, i.e., the determination of the drift velocity, of the amplification gain and of the electron absorption, is performed by the analysis of the time distribution of the average charge per track as was described in section 3.2. A special trigger line ($\sim 2\%$ of the events) was used to select the tracks traversing in the z direction (i.e., along the drift time) without biasing the time distribution.

Fig. 10 and Fig. 11 show that there was no significant gas deterioration over the two weeks in the beam. The small features that can be seen in the time charts (Fig. 11) are associated with changes in the gamma-beam energy and/or of the laser pulsing rate, meaning that these small biases are related to the measurement, not to the quantity measured. The gas gain and the drift velocity were found to be sufficiently stable and the electron absorption due to either leaks or outgassing was found to be sufficiently small that we didn't have to renew the gas.

5. Conclusions and perspectives

A gas TPC is the instrument suited to covering the performance gap in cosmic gamma-ray detection in the MeV-GeV range. We have built a demonstrator that includes a micromegas+GEM amplification system. We have performed an experimental campaign with this demonstrator using the high-flux, quasi-monochromatic, polarised photon beam at NewSUBARU. Tests that were performed during data taking indicate an excellent detector performance.

We have more than 1 TB of data ($> 6 \times 10^7$ events, a large fraction of which is estimated to be gamma conversions in the gas) to analyze so that we can study the gamma conversion to e^+e^- pairs and, in particular, measure the low energy polarization asymmetry, and characterize the performance of the demonstrator both as a gamma telescope and as a gamma polarimeter. Further development is ongoing to meet the constraints of a space environment [14], in particular, tests on the behaviour of the detector in space with a dedicated trigger. The next step will then be to verify its operation with a balloon flight.

6. Acknowledgments

This work is funded by the P2IO LabEx (ANR-10-LABX-0038) in the framework “Investissements d’Avenir” (ANR-11-IDEX-0003-01) managed by the French National Research Agency (ANR), and directly by the ANR (ANR-13-BS05-0002).

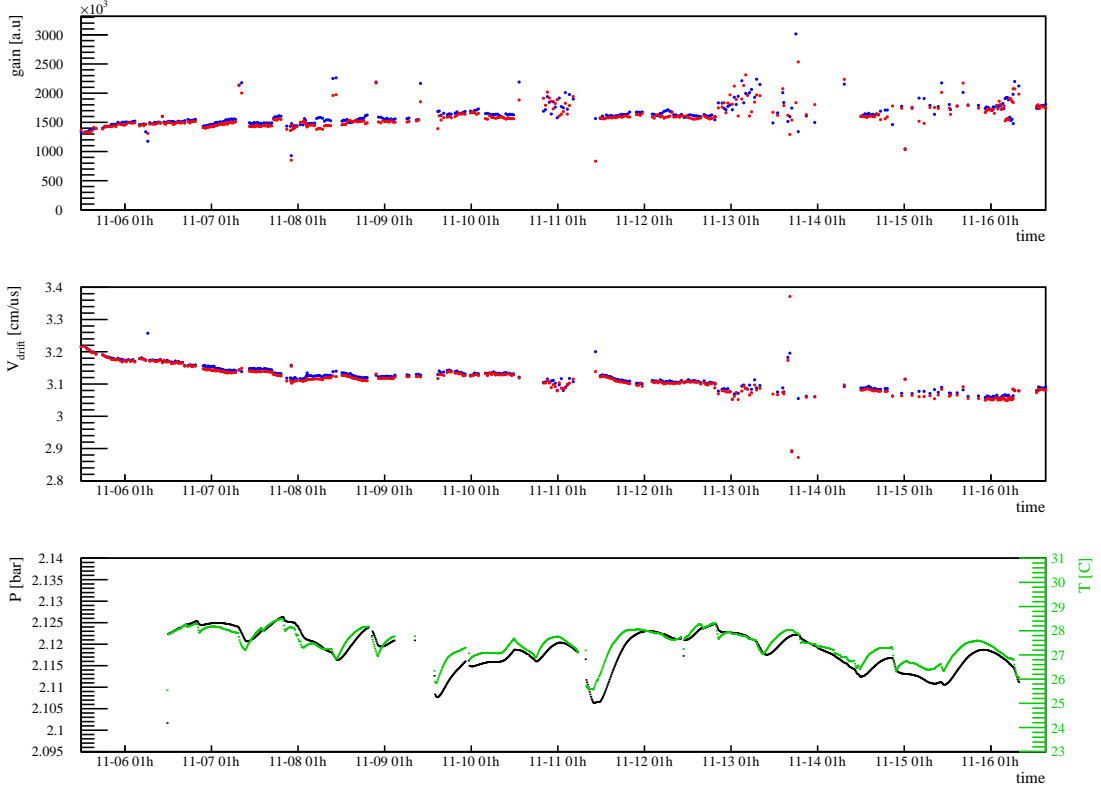


Figure 11. Time variation of the gain, estimated by the average charge per track, corrected for the track angle that is normalized to 30 cm track length, the drift velocity (x in red, y in blue) and the pressure (black) and temperature (green) of the gas.

This work was performed by using NewSUBARU-GACKO (Gamma Collaboration Hutch of Konan University).

References

- [1] D. Eichler, A. Levinson, *Polarization of GRB via scattering off a relativistic sheath*, *Astrophys. J.* **596**, L147 (2003). [astro-ph/0306360].
- [2] H. Zhang and M. Böttcher, *X-Ray and Gamma-Ray Polarization in Leptonic and Hadronic Jet Models of Blazars*, *Astrophys. J.* **774**, 18 (2013) [arXiv:1307.4187 [astro-ph.HE]].
- [3] M. Forot, P. Laurent, I. A. Grenier, C. Gouiffes and F. Lebrun, “Polarization of the Crab pulsar and nebula as observed by the Integral/IBIS telescope,” *Astrophys. J.* **688**, L29 (2008) [arXiv:0809.1292 [astro-ph]].
- [4] H. Bloemen, “Diffuse galactic gamma-ray emission,” *Ann. Rev. Astron. Astrophys.* **27** (1989) 469.
- [5] M. Ackermann *et al.* [Fermi-LAT Collaboration], *The Fermi Large Area Telescope On Orbit: Event Classification, Instrument Response Functions, and Calibration*, *Astrophys. J. Suppl.* **203**, 4 (2012) [arXiv:1206.1896 [astro-ph.IM]].
- [6] D. Bernard, *TPC in gamma-ray astronomy above pair-creation threshold*, *Nucl. Instrum. Meth. A* **701**, 225 (2013) [Erratum-ibid. *A* **713**, 76 (2013)] [arXiv:1211.1534 [astro-ph.IM]].
- [7] D. Bernard, *Polarimetry of cosmic gamma-ray sources above e^+e^- pair creation threshold*, *Nucl. Instrum. Meth. A* **729**, 765 (2013) [arXiv:1307.3892 [astro-ph.IM]].
- [8] Mattox, J. R., Mayer-Hasselwander, H. A., Strong, A. W., *Analysis of the COS B data for evidence of linear polarization of VELA pulsar gamma rays*, *Astrophys. J.* 363 (1990) 270.
- [9] D. Bernard, *HARPO - A Gaseous TPC for High Angular Resolution Gamma-Ray Astronomy and Polarimetry from the MeV to the TeV*, *Nucl. Instrum. Meth. A* **718**, 395 (2013). [arXiv:1210.4399 [astro-ph.IM]].

- [10] F. Sauli, *GEM: A new concept for electron amplification in gas detectors*, Nucl. Instrum. Meth. A **386**, 531 (1997).
- [11] Y. Giomataris, P. Rebourgeard, J. P. Robert and G. Charpak, *MICROMEGAS: A high-granularity position-sensitive gaseous detector for high particle-flux environments*, Nucl. Instrum. Meth. A **376**, 29 (1996).
- [12] P. Baron, D. Calvet, E. Delagnes *et al.*, *AFTER, an ASIC for the readout of the large T2K time projection chambers*, IEEE Trans. Nucl. Sci. **55**, 1744 (2008).
- [13] D. Calvet, “A Versatile Readout System for Small to Medium Scale Gaseous and Silicon Detectors”, IEEE Transactions on Nuclear Science 61 (2014) 675.
- [14] D. Bernard *et al.*, Presented at SPIE2014. Proc SPIE 9144 M. [arXiv:1406.4830 [astro-ph.IM]].
- [15] S. Amano *et al.*, *Several-MeV γ -ray generation at NewSUBARU by laser Compton backscattering*, Nucl. Instrum. Meth. A **602** 2009 337.
- [16] Ph. Gros, *HARPO - TPC for High Energy Astrophysics and Polarimetry from the MeV to the TeV*, TIPP 14 3rd Technology and Instrumentation in Particle Physics conference, 2-6 June 2014 Amsterdam, Proceedings PoS(TIPP2014)133.
- [17] M. Weisskopf, *X-ray Polarimetry: from the early days to an outlook for the future*, X-ray polarisation in astrophysics, August 25-28, Stockholm, Sweden.
- [18] B. Genolini *et al.*, *PMm2: Large photomultipliers and innovative electronics for the next-generation neutrino experiments*, Nucl. Instrum. Meth. A **610** (2009) 249 [arXiv:0811.2681 [physics.ins-det]].
- [19] S. Conforti Di Lorenzo *et al.*, *PARISROC, an autonomous front-end ASIC for triggerless acquisition in next generation neutrino experiments*, Nucl. Instrum. Meth. A **695** (2012) 373.